

Online Domain-aware LLM Decoding for Continual Domain Evolution

Mohammad Abu-Shair and Weishi Shi

University of North Texas, Denton, TX, USA

Abstract. LLMs are typically fine-tuned offline on domain-specific data, assuming a static domain. In practice, domain knowledge evolves continuously through new regulations, products, services, and interaction patterns. Retraining or fine-tuning LLMs for every new instance is computationally infeasible. Additionally, real-world environments also exhibit temporal dynamics with shifting data distributions. Disregarding this phenomenon, commonly referred to as concept drift, can significantly diminish a model’s predictive accuracy. This mismatch between evolving domains and static adaptation pipelines highlights the need for efficient, real-time adaptation without costly retraining. In response, we introduce Online Domain-aware Decoding framework (*ODD*). *ODD* performs probability-level fusion between a base LLM and a prefix-tree prior, guided by adaptive confidence modulation using disagreement and continuity signals. Empirical evaluation under diverse drift scenarios demonstrates that *ODD* consistently surpasses LLM-Greedy and LLM-Temp Scaled across all syntactic and semantic NLG metrics. It yields an absolute ROUGE-L gain of **0.065** and a **13.6%** relative improvement in Cosine Similarity over the best baseline. These results demonstrate *ODD*’s robustness to evolving lexical and contextual patterns, making it suitable for dynamic LLM applications.

Keywords: Inference-Time Adaptation · Online Inference · Decoding Strategies · Large Language Models · Concept Drift · Prefix Tree

1 Introduction

Large Language Models (LLMs) such as GPT-3 [5], PaLM [6], and LLaMA [31] excel in many NLP tasks due to large-scale pretraining and adaptation techniques like supervised fine-tuning and RLHF [24]. While effective for generalization, these offline strategies are limited when deployed in specialized domains that require strict adherence to dynamic, evolving knowledge. For example, LLM-powered assistants in customer support and decision-making [36] demand consistency, factual accuracy, and domain compliance. Yet both general-purpose and fine-tuned models often hallucinate or deviate from requirements when domain knowledge changes [11, 21].

Although pretrained LLMs are typically fine-tuned on *domain-specific* datasets, this adaptation is performed *offline* and assumes a static domain. In practice,

domain knowledge evolves through new terminology, updated products, changing regulations, shifting pricing, modified services, and emerging user intents, causing *concept drift* [9]. Because modern LLMs are expensive to retrain, frequent fine-tuning is impractical, creating a barrier to real-time adaptation [30]. This gap underscores the need for efficient, real-time learning approaches [9,8]. Despite their versatility, LLMs face practical challenges in dynamic environments. Repeated fine-tuning or retraining is computationally expensive and time-consuming [37], risks *catastrophic forgetting* [8], and may violate *data privacy and regulatory* constraints. These limitations motivate inference-time mechanisms that incorporate new domain knowledge without modifying model weights.

Although extensive research exists, current decoding and adaptation strategies exhibit fundamental limitations for online domain adaptation. *Logit-based decoding control* avoids retraining but often requires auxiliary controllers or extra forward/backward passes per token, providing only local control that degrades under domain shift. *Prefix- and context-aware decoding* methods impose rigid constraints or rely on static priors, lacking mechanisms for temporal or drift-aware adaptation. *Retrieval-guided decoding* introduces significant latency overhead and relies on the freshness and maintenance of external knowledge indices. Finally, *parameter-efficient adaptation* and model-editing techniques require offline, task-specific training or permanent modification of model weights, preventing real-time, zero-training inference adaptation.

These limitations highlight the need for a drift-aware framework that enables online adaptability without retraining, auxiliary models, or external retrieval. In response, we introduce *ODD*, a lightweight inference-time framework that dynamically aligns generation with evolving domain knowledge. *ODD* performs probability-level fusion between the base LLM and an online Trie prior, guided by adaptive *confidence* modulation through *disagreement* and temporal *continuity* signals. The source code is available at our GitHub repository [2].

2 Related Work

Logit-Based Decoding Control: Decoding control adjusts logits during inference to steer generation. *Auxiliary controllers* (e.g., *PPLM* [7], *GeDi* [13]) rely on external models, while *internal methods* (*DExperts* [19], *Self-Debiasing* [29], *FUDGE* [33]) use contrastive or self-generated signals. These techniques avoid full retraining but demand auxiliary passes and offer only short-term control that fails under domain shift. **Prefix and Context-Aware Decoding:** Prefix-aware decoding guides next-token prediction using the generated context. *Hard constraints* (e.g., *Constrained Beam Search* [1]) enforce required phrases, while *soft priors* (e.g., *Dynamic Vocabulary Selection/Pruning* [16,32]) reweight token probabilities based on prefix-conditioned candidates. **Retrieval- and Knowledge Guided Decoding** These methods retrieve external evidence conditioned on the prefix and integrate it to bias next-token prediction. *kNN-LM* [12] interpolates the base distribution with nearest-neighbor targets, while generative models such as *RAG* [15] and *RETRO* [4] condition decoding on retrieved

documents for fact-aware output. *Knowledge-Infused Decoding* [20] instead injects knowledge signals directly into the logits. These methods provide strong factual grounding but incur retrieval latency and depend on index freshness.

Parameter-Efficient Adaptation and Model Editing *Parameter-Efficient Adaptation (PEA)* trains lightweight components while freezing the base LLM. Methods such as *Prefix-Tuning* [17], *Prompt Tuning* [14], and *LoRA* [10] adapt internal representations through task-specific training. In contrast, *Model Editing* techniques like *ROME* [22] and *MEMIT* [23] modify model parameters directly to embed factual updates. Both lines of work complement decoding-based approaches that guide inference externally without altering model weights.

3 Problem Settings

Let \mathcal{V} be the vocabulary and $\mathbf{x} = (x_1, \dots, x_T)$ be a sequence. Given a prefix $\pi_t = (x_1, \dots, x_t)$, the LLM (parameterized by θ) estimates the next token distribution $P_\theta(y \mid \pi_t)$ from its output logit vector $\mathbf{z}_t \in \mathbb{R}^{|\mathcal{V}|}$. We define the base distribution as $q_t^{\text{LM}} = \text{softmax}(\mathbf{z}_t)$, where $q_t^{\text{LM}} = P_\theta(\cdot \mid \pi_t)$. LLMs are typically fine-tuned offline assuming a stationary data distribution. In real-world scenarios, domain knowledge evolves continuously, with new sequences arriving sequentially in an unbounded stream. This non-stationary distribution leads to *concept drift*. Formally, drift occurs when $\exists \pi_t, y : p_t(y \mid \pi_t) \neq p_{t+1}(y \mid \pi_t)$, meaning the true distribution over next-token continuations changes over time. This challenge requires maintaining LLM performance in online environments. This necessitates adapting the LLM’s next-token distribution in real time to evolving domain knowledge, critically *avoiding parameter updates*. Our objective is to construct an adapted distribution \tilde{q}_t that balances fidelity to the base q_t^{LM} (*stability*) with responsiveness to domain evidence from the *Prefix Trie* (*adaptability*). Formally, the objective balances *stability* to the base model with *adaptability* to domain-specific signals extracted from the Trie. Let q_t^{Pn} denote the Trie-induced prior derived from the feature vector ϕ_t . We express this trade-off as:

$$\tilde{q}_t = \arg \min_{q \in \Delta^{|\mathcal{V}|}} \left\{ \mathcal{D}(q \parallel q_t^{\text{LM}}) + \mathcal{D}(q \parallel q_t^{\text{Pn}}) \right\},$$

where $\mathcal{D}(\cdot \parallel \cdot)$ is a divergence measure capturing stability, q_t^{Pn} encodes the domain-specific Trie features through ϕ_t , and the formulation jointly encourages adherence to the base model while aligning with evolving domain evidence.

4 Method

The proposed decoding strategy augments the finetuned base LLM with domain priors extracted from the Prefix Trie. At each generation step, the strategy constructs two distributions: the LLM’s base distribution and the Prefix Trie prior, which captures structural statistics (*frequency, recency, and length*) from the online data stream. These distributions are combined through an adaptive fusion mechanism using a *confidence-based* weighting factor, which is dynamically

determined by *disagreement* and temporal *continuity* signals. This fusion leverages the LLM’s finetuned domain knowledge while incorporating the Trie’s fast, online updates, circumventing the high cost of continual finetuning. To establish a strong domain foundation, we *finetune a pretrained LLM* on target data. This model serves as the base for our approach, supplying the output logits ($\mathbf{z}_t \in \mathbb{R}^{|V|}$) that initiate the fusion process at every prediction step.

4.1 Online Prefix Tree Construction

The Prefix Tree (Trie) is continuously updated with evolving domain knowledge using an n -gram scheme that inserts all token sequences up to length N . This keeps both short and long domain phrases current and directly available for next-token prediction.

Each trie entry stores three features: *Recency* (**R**), *Length* (**L**), and *Frequency* (**F**). **R** tracks when a continuation last appeared, **L** measures how closely its span matches the query prefix, and **F** counts how often it occurs. These features are updated at each node whenever new instances appear, allowing the trie to function as a dynamic scoring mechanism that reflects the temporal, structural, and statistical relevance of domain knowledge.

Consider two domain sequences inserted into the n -gram Trie: the older \mathbf{s}_1 (“Activate your plan 4G”) and the more recent \mathbf{s}_2 (“Please activate your plan 5G”). *For clarity, this illustration uses word-level nodes, while the actual implementation constructs the Trie over token-level sequences.* The node-level features (**F**, **L**, **R**) capture the structural, statistical, and temporal properties of these sequences (see Figure 1): **Recency** (**R**): Records the most recent observation time. The “4G” leaf carries an earlier timestamp, whereas “5G” reflects the newer update, enabling recency-aware scoring. **Length** (**L**): Denotes the depth of the token in the sequence, rewarding longer, more specific matches (e.g., $L = 5$ for the full “5G” path). **Frequency** (**F**): Counts the number of times a prefix appears. For example, the shared path “activate → your → plan” has $\mathbf{F} = 2$.

4.2 Candidate Tokens Scoring Mechanism

At each decoding step t , the method queries the trie to construct a candidate set \mathcal{C} (unique next tokens with highest feature score), and computes a probability distribution $q_t^{\mathcal{P}_n}$ over \mathcal{C} . Given the prefix π_t , *all matching suffixes* in the Trie \mathcal{P}_n are queried to populate the candidate set \mathcal{C} with unique next tokens y and their associated feature vectors $\phi = (\mathbf{F}, \mathbf{L}, \mathbf{R})$. To reduce bias from large token counts, the **Frequency** feature is transformed as $\mathbf{F}'' = \log(1 + \mathbf{F})$. Each candidate’s

```
(root)
  +- activate (F=2, L=1, R=1759263260)
  |  +- your (F=2, L=2, R=1759263260)
  |  |  +- plan (F=2, L=3, R=1759263260)
  |  |  |  +- 4G (F=1, L=4, R=1758658460)
  |  |  |  +- 5G (F=1, L=4, R=1759263260)
  +- your (F=2, L=1, R=1759263260)
  |  +- plan (F=2, L=2, R=1759263260)
  |  |  +- 4G (F=1, L=3, R=1758658460)
  |  |  +- 5G (F=1, L=3, R=1759263260)
  +- plan (F=2, L=1, R=1759263260)
  |  +- 4G (F=1, L=2, R=1758658460)
  |  +- 5G (F=1, L=2, R=1759263260)
  +- please (F=1, L=1, R=1759263260)
  |  +- activate (F=1, L=2, R=1759263260)
  |  |  +- your (F=1, L=3, R=1759263260)
  |  |  |  +- plan (F=1, L=4, R=1759263260)
  |  |  |  +- 5G (F=1, L=5, R=1759263260)
```

Fig. 1: n -gram Trie with Frequency (**F**), Length (**L**), and Recency (**R**).

preliminary score is computed from the normalized feature tuple $(\mathbf{F}', \mathbf{L}', \mathbf{R}')$. Frequency is normalized across the candidate set using $\mathbf{F}' = \mathbf{F}'' / \max_{y' \in \mathcal{C}} \mathbf{F}''$, ensuring that frequent continuations do not dominate the scoring range and remain comparable to the other normalized features. **Length** is normalized with respect to the current prefix depth, $\mathbf{L}' = \mathbf{L} / |\pi_t|$, ensuring proportional credit for contextual alignment rather than rewarding overly long sequences. **Recency** is modeled via an exponential decay, $\mathbf{R}' = \exp(-\Delta/\Delta_{\max})$, where Δ denotes the recency gap; here, $\Delta_{\max} = \max_{y' \in \mathcal{C}} \Delta(y')$ ensures well-defined normalization over the candidate set. This assigns $\mathbf{R}' = 1$ to the most recent continuation while preserving a nonzero contribution for older candidates. The final score for each candidate token is obtained through a weighted linear combination, $\text{score}(y) = \langle \boldsymbol{\lambda}, (\mathbf{F}', \mathbf{L}', \mathbf{R}') \rangle$. The non-negative weight vector $\boldsymbol{\lambda} = (\lambda_R, \lambda_L, \lambda_F)$ (summing to 1) is configurable, allowing users to prioritize specific domain statistics (e.g., *Recency*). This formulation yields an interpretable final score in the range $(0, 1]$, reflecting the candidate’s overall strength. The resulting scores are later converted into a valid probability distribution $q_t^{\mathcal{P}_n}$ by top-preserving normalization over the candidate set \mathcal{C} , assigning zero mass to tokens outside \mathcal{C} .

4.3 Probability Distribution Preparation and Calibration

The candidate scores are first mapped to the sparse Trie distribution $(q_t^{\mathcal{P}_n})$ using a *top-preserving normalization* scheme (Line 17, Algorithm 1), which retains the maximum score (S_{\max}) while proportionally distributing the remaining mass to ensure a valid probability sum. Since the neural q_t^{LM} and statistical $q_t^{\mathcal{P}_n}$ distributions operate on different confidence scales, we apply *adaptive temperature scaling* prior to interpolation. This mechanism dynamically adjusts the LLM’s sharpness (via T_t^* in Equation 1) until its peak probability precisely matches that of $q_t^{\mathcal{P}_n}$ (Equation 2). This crucial calibration eliminates scale bias between the experts, preparing them for the final dynamic fusion ($\tilde{q}_t = \gamma_t q_t^{\text{LM}} + (1 - \gamma_t) q_t^{\mathcal{P}_n}$). Because temperature scaling is a monotonic, rank-preserving transformation of logits, it adjusts only the sharpness of the distribution and therefore modifies probability mass in a controlled manner.

$$T_t^* = \arg \min_{T > 0} \left| \max_{y \in V} \text{softmax}\left(\frac{\mathbf{z}_t}{T}\right) - \max_{y \in V} q_t^{\mathcal{P}_n}(y) \right| \quad (1)$$

$$\max_{y \in V} \text{softmax}\left(\frac{\mathbf{z}_t}{T_t^*}\right) = \max_{y \in V} q_t^{\mathcal{P}_n}(y) \quad (2)$$

A unique solution for T_t always exists because $\max \text{softmax}(\mathbf{z}_t/T)$ is a continuous, strictly monotonic function of T , and we obtain T_t via a 1D monotonic root-finding method (bisection).

4.4 Establishing Distributions Confidence

The adaptive interpolation weight γ_t is computed dynamically at each step, reflecting the current certainty of the two experts. When the LLM is confident, γ_t is high, increasing its influence, and vice versa. The base *LLM confidence* (c_{LM}) is quantified using its *normalized entropy* ($H(\mathbf{q}_t^{\text{LM}})$) (Lines 15, and 16 Algorithm

Algorithm 1 *ODD*: Online Domain-Aware Decoding

```

1: Input:  $\mathbf{z}_t \in \mathbb{R}^{|V|}$ ;  $\mathcal{P}_n = \{p \mapsto n(p) : \phi \mid \phi = (\mathbf{F}, \mathbf{L}, \mathbf{R})\}; \pi_t = (x_1, \dots, x_t); \theta = \{\lambda\}$ 
       $\triangleright \lambda = (\lambda_{\mathbf{F}}, \lambda_{\mathbf{L}}, \lambda_{\mathbf{R}}), \sum_i \lambda_i = 1; x_i \in V$ 
2:  $\mathcal{C} \leftarrow \{\}$ 
3: for each suffix  $s$  of  $\pi_t$  do
4:   for each  $(y, \phi) \in \text{NextTokens}(s, \mathcal{P}_n)$  do
5:      $\mathbf{f}'' = \log(1 + \mathbf{f}); \mathbf{f}' \leftarrow \frac{\mathbf{f}''}{\max_{y' \in \mathcal{C}} \mathbf{f}''}; \mathbf{l}' \leftarrow \frac{\mathbf{l}}{|\pi_t|}; \mathbf{r}' \leftarrow \exp\left(-\frac{\Delta}{\Delta_{\max}}\right)$ 
6:      $\text{score}(y) \leftarrow \langle \lambda, (\mathbf{f}', \mathbf{l}', \mathbf{r}') \rangle$   $\triangleright \text{score}(y) \in (0, 1]$ 
7:     if  $y \notin \mathcal{C}$  or  $\text{score}(y) > \text{score}_{\mathcal{C}}(y)$  then
8:       update  $\mathcal{C}$  with  $(y, \text{score}(y))$ 
9:     end if
10:   end for
11: end for
12:  $q_t^{\text{LM-base}} \leftarrow \text{softmax}(\mathbf{z}_t)$   $\triangleright \text{LLM distribution (before temp adjustment)}$ 
13:  $H \leftarrow -\sum_{y \in V} q_t^{\text{LM-base}}[y] \log q_t^{\text{LM-base}}[y]$ 
14:  $c_{\text{LM}} \leftarrow 1 - \frac{H}{H_{\max}}$   $\triangleright H_{\max} \leftarrow \log |V|$ 
15:  $q_t^{\mathcal{P}_n}(y) \leftarrow S_{\max} \mathbf{1}_{\{y=y_{\max}\}} + \frac{(1 - S_{\max}) \text{score}(y)}{\sum_{y' \in \mathcal{C} \setminus \{y_{\max}\}} \text{score}(y')}$   $\triangleright S_{\max} = \max_{y \in \mathcal{C}} \text{score}(y)$ 
16:  $c_{\text{trie}} \leftarrow \max_{y \in V} q_t^{\mathcal{P}_n}[y]$ 
17:  $q_t^{\text{LM}} \leftarrow \text{softmax}\left(\frac{\mathbf{z}_t}{T_t}\right)$   $\triangleright \text{LLM distribution (after adaptive temperature)}. T_t \text{ is adaptive temperature chosen s.t. } \max q_t^{\text{LM}} = S_{\max}$ 
18:  $c'_{\text{LM}} \leftarrow c_{\text{LM}}(1 - \Omega^2)$   $\triangleright \Omega: \text{disagreement using Top-}k \text{ (here } k = 5\text{)}$ 
19:  $c'_{\text{trie}} \leftarrow c_{\text{trie}} + (1 - c_{\text{trie}}) c_{\text{trie}}^2 \Gamma$   $\triangleright \Gamma \text{ is continuity}$ 
20:  $\gamma_t \leftarrow \frac{c'_{\text{LM}}}{c'_{\text{LM}} + c'_{\text{trie}}}$ 
21:  $y^* \leftarrow \arg \max_{y \in V} \left( \gamma_t q_t^{\text{LM}}[y] + (1 - \gamma_t) q_t^{\mathcal{P}_n}[y] \right)$ 
22:  $\pi_{t+1} \leftarrow (\pi_t, y^*)$ 
23: return  $\pi_{t+1}$ 

```

1), resulting in a scale-invariant measure $c_{\text{LM}} \in [0, 1]$ where low entropy (high certainty) results in c_{LM} near 1. The *Trie confidence* (c_{trie}) is simply defined as the *maximum probability* assigned to its top-preserving candidate (Line 18, Algorithm 1). Since $q_t^{\mathcal{P}_n}$ is constructed to emphasize its strongest candidate, this maximum value naturally indicates the distribution's confidence.

4.5 Rewarding and Penalizing Distribution Confidence

The intrinsic confidences (c_{LM} and c_{trie}) are refined using two context-aware factors: **Disagreement** (Ω_t) and **Continuity** (Γ_t). Ω_t measures how differently the two experts rank their top- k tokens (we use $k = 5$ in all experiments), while Γ_t captures temporal agreement through r_t , the number of consecutive steps in which both experts select the same top token. We form the union set \mathcal{I}_k from the top- k tokens of each distribution and normalize them over this set (Equations 3–4). JSD is computed (Equation 5), and Ω_t follows from its square

root (Equation 6), with larger values reducing the LLM’s confidence. Γ_t is an exponential function of r_t (Equation 7), rewarding the Trie when agreement is consistent. The final confidences (c'_{LM} , c'_{trie}) combine these factors, with Ω_t penalizing the LLM and Γ_t amplifying the Trie.

$$p(y) = \frac{q_t^{\text{LM}}[y]}{\sum_{y' \in \mathcal{I}_k} q_t^{\text{LM}}[y']} \quad (3) \quad q(y) = \frac{q_t^{\mathcal{P}_n}[y]}{\sum_{y' \in \mathcal{I}_k} q_t^{\mathcal{P}_n}[y']} \quad (4)$$

$$\text{JSD}(p, q) = \frac{1}{2} \sum_{y \in \mathcal{I}_k} [p(y) \log \frac{p(y)}{m(y)} + q(y) \log \frac{q(y)}{m(y)}], \quad m(y) = \frac{1}{2}(p(y) + q(y)) \quad (5)$$

$$\Omega_t = \min(1, \sqrt{\text{JSD}(p, q)}) \quad (6) \quad \Gamma_t = 1 - \exp\left(-\frac{r_t}{3}\right) \quad (7)$$

4.6 Next Token Prediction

Finally, the adaptive interpolation coefficient (γ_t) is computed from the adjusted confidences, preserving **relative confidence** by ensuring $\gamma_t = c'_{\text{LM}} / (c'_{\text{LM}} + c'_{\text{trie}})$. This coefficient is used to form the final adapted probability distribution (\tilde{q}_t) as a convex combination of the LLM’s linguistic prior and the Trie’s likelihoods: $\tilde{q}_t(y) = \gamma_t q_t^{\text{LM}}(y) + (1 - \gamma_t) q_t^{\mathcal{P}_n}(y)$. At each step, the next token y_t^* is selected by maximizing this mixed distribution, $y_t^* = \arg \max_{y \in V} \tilde{q}_t(y)$, guaranteeing a principled balance between linguistic fluency and domain-specific recurrence.

4.7 Time and Memory Complexity

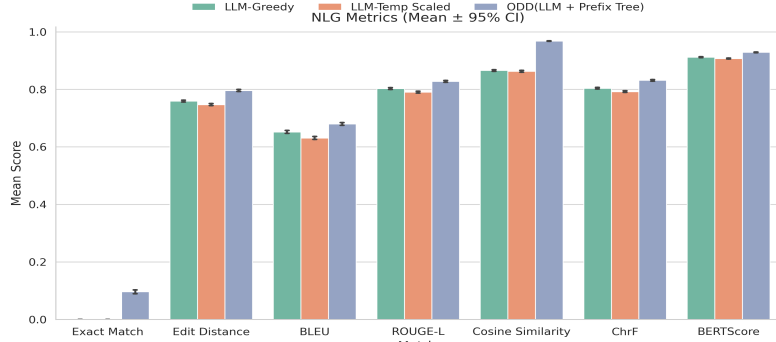
The operational efficiency of the Trie is fundamental to *ODD*’s lightweight, inference-time design. Defining $L = |\pi_t|$ as the prefix length, **online insertion** remains linear, $\mathcal{O}(L)$, as each token corresponds to one node traversal. The **all-suffix retrieval** procedure explores every suffix of the prefix sequence π_t , resulting in a worst-case complexity of $\mathcal{O}(L^2)$. Importantly, both insertion and retrieval are **independent of the number of stored sequences (N)**, ensures decoding latency remains bounded as the domain knowledge base expands.

Memory-wise, the Trie allocates one node per distinct token position. The worst-case memory complexity is $\mathcal{O}(L_{\text{total}})$, where L_{total} is the total number of inserted tokens. However, because *ODD* indexes only compact, tokenized place-holders rather than full conversational texts, the trie’s size grows proportionally to the number of unique placeholder patterns. The resulting **empirical memory complexity** is $\mathcal{O}(U)$, where U denotes the number of distinct placeholder prefixes, which is typically far smaller than the theoretical bound. Empirical profiling confirms that Trie updates and retrievals introduce sub-millisecond latency per decoding step, consistent with the theoretical bounds above.

5 Experiments

5.1 Datasets, Evaluation Metric & Baseline

We use the *Bitext Telco LLM Chatbot Training Dataset* ($\approx 26,000$ samples, 26 intents), which **natively contains placeholder tokens**. We substitute these placeholders to create controlled *abrupt*, *incremental*, and *gradual* concept-drift

Fig. 2: NLG Metrics (Mean \pm 95% CI) under abrupt drift

scenarios. Figure [3] illustrates the *Bitext* dataset under the *abrupt*, *incremental*, and *gradual* placeholder drift scenario. To measure the overall distributional drift, we track lexical and semantic shifts using *Jensen-Shannon Distance (JSD)* to assess lexical divergence, *Cosine Distance* to capture semantic drift on sentence embeddings, *BERTScore F1* to assess contextual alignment, and *Maximum Mean Discrepancy (MMD)*. To evaluate *model performance* under drift, we compare *ODD* against baseline decoders using: (a) lexical similarity (Exact Match[27], NED [34], BLEU [25], ChrF [26]), (b) structural coherence (ROUGE-L [18]), and (c) semantic alignment (Cosine Similarity [28], BERTScore [35]). The dataset involves placeholder tokens, a common convention in public and real-world NLP datasets such as MultiWOZ and customer-support corpora, used to represent dynamic and evolving entities (for example, product names or account identifiers). This placeholder drift provides a practical and realistic proxy for real-world distribution shift. Importantly, *ODD* is not limited to placeholders; the Trie incorporates any newly observed tokens or patterns, enabling domain-agnostic adaptation. Both calibration and confidence computation add less than 0.2 ms overhead per decoding step, preserving real-time inference.

We benchmark our method against two well-recognized decoding strategies: *LLM-Greedy* and *LLM-Temp Scaled*. We restrict our baselines to decoding-only methods because our setting assumes zero-training, inference-time online adaptation with no external retrieval or model updates. Retrieval-augmented approaches (e.g., RAG, kNN-LM), prefix-constrained decoding (e.g., Constrained Beam Search, CBS), and parameter-efficient adaptation methods require external memory, static constraints, or offline training, making them incompatible with our real-time drift scenario.

5.2 Performance Analysis under Drift

Figure 2 reports mean **syntactic** and **semantic** performance under the *abrupt* scenario across the decoding strategies: *LLM-Greedy*, *LLM-Temp Scaled*, and *ODD*. The proposed *ODD* consistently outperforms both baselines, with the largest gains in semantic alignment. It achieves a Cosine Similarity of **0.968** versus **0.865** and **0.863**, and a BERTScore of **0.928** versus **0.911** and **0.907**.

Table 1: Decoding Strategies Performance Under Drift

E.M. Exact Match, E.D. Edit Distance, Cos-Sim. Cosine Similarity, BERT. BERTScore.

Strategy	E.M.	E.D.	BLEU	ROUGE-L	Cosine Sim.	ChrF	BERT.
Abrupt Drift							
Greedy	0	0.759	0.652	0.803	0.865	80.374	0.911
Temp Scaled	0	0.747	0.631	0.790	0.863	79.199	0.907
ODD	0.096	0.796	0.679	0.828	0.968	83.147	0.928
Incremental Drift							
Greedy	0	0.740	0.600	0.790	0.865	78.304	0.908
Temp Scaled	0	0.725	0.574	0.775	0.862	76.886	0.902
ODD	0.052	0.803	0.682	0.838	0.976	83.826	0.935
Gradual Drift							
Greedy	0	0.702	0.555	0.760	0.855	74.031	0.890
Temp Scaled	0	0.687	0.529	0.745	0.853	72.710	0.885
ODD	0.037	0.790	0.663	0.825	0.971	82.824	0.928

for *LLM-Greedy* and *LLM-Temp Scaled*, respectively. These results confirm *ODD* ’s robustness in preserving meaning and coherence under abrupt lexical shifts.

Table 1 reports mean **syntactic** and **semantic** performance for *LLM-Greedy*, *LLM-Temp Scaled*, and *ODD*. Under *incremental* drift, *ODD* shows the strongest stability, achieving a Cosine Similarity of **0.976** versus **0.865** and **0.862**, and a BERTScore of **0.935** versus **0.908** and **0.902**. It also attains the best syntactic alignment (ChrF **83.83** vs. **78.30** and **76.89**). Under *gradual* drift, *ODD* again yields the highest semantic scores, with Cosine Similarity **0.971** (vs. **0.855** and **0.853**) and BERTScore **0.928** (vs. **0.890** and **0.885**). For *syntactic* alignment, *ODD* achieves the highest ChrF (**82.82** vs. **74.03** and **72.71**), with BLEU and ROUGE-L showing the same trend. These results confirm *ODD* ’s resilience to gradual lexical drift while preserving both form and meaning.

Across all scenarios, *ODD* consistently outperformed the baselines in *syntactic* and *semantic* quality. Under the most challenging *gradual* drift, *ODD* achieved a ROUGE-L of 0.825 (an absolute gain of **0.065** over the strongest baseline) and a Cosine Similarity of 0.971 (a relative improvement of **13.6%**). These gains, consistent across abrupt and incremental drift, demonstrate *ODD* ’s ability to maintain syntactic structure and semantic coherence as lexical distributions shift.

To illustrate the **qualitative** impact of *ODD*, we highlight an example from the abrupt drift scenario. After the drift, the ground truth introduces a new plan (“Talk + Net Pack”) and brand (“TalkNow Crew”). Both baselines continue generating outdated Concept 1 templates such as “To sign up for a Mobile Voice and Data Communication Service...,” failing to reflect the new domain state. In contrast, *ODD* adapts correctly and produces “To sign up for a Talk + Net Packet plan with TalkNow Crew...,” aligning with the drifted concept while maintaining structural consistency. This example shows how *ODD* updates in real time while baseline decoders remain anchored to pre-drift patterns.

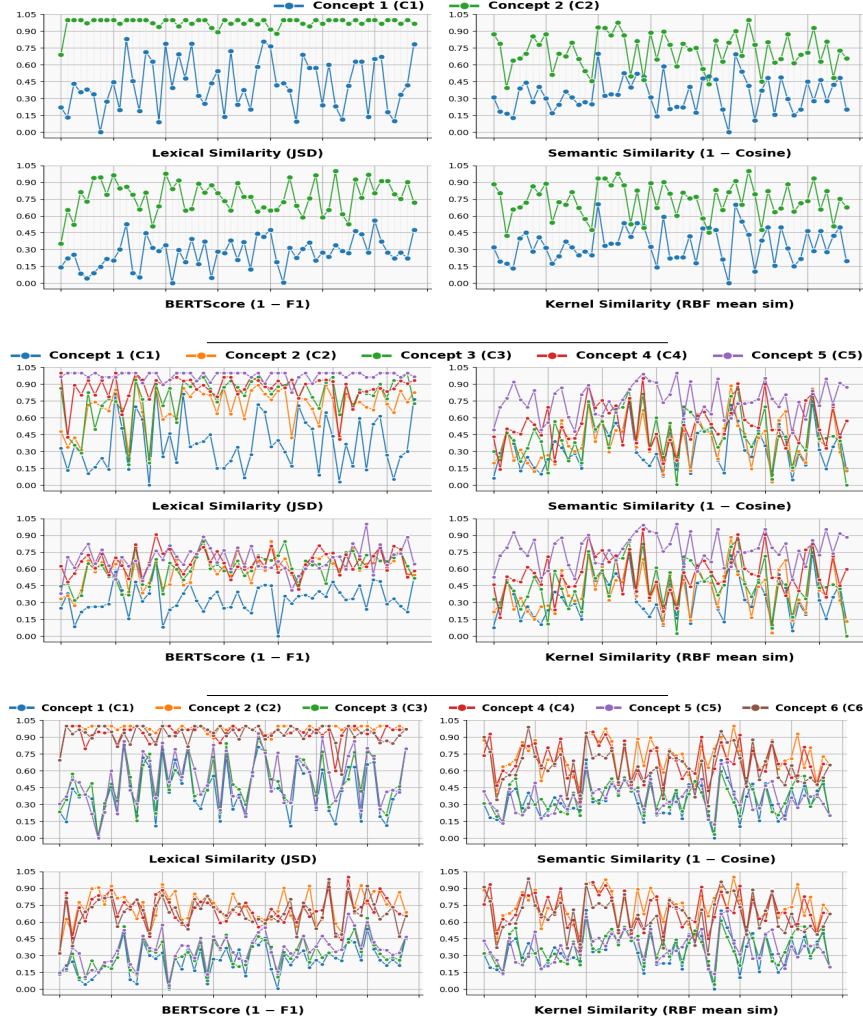


Fig. 3: Concept drift in placeholders: (top) Abrupt, (middle) Incremental, (bottom) Gradual.

5.3 Ablation Summary & Reproducibility

Ablation Summary. Using both *disagreement* (Ω_t) and *continuity* (Γ_t) jointly produced the most stable behavior; enabling only one signal reduced robustness. *Temperature calibration* was also critical, as disabling it caused confidence-scale mismatches between the LLM and Trie distributions. Trie feature weights were fixed to *uniform values* ($\lambda_F = \lambda_L = \lambda_R = 1/3$), which yielded stable performance; exploring alternative weightings remains future work.

Reproducibility. All experiments used the `gpt2-medium` model (355M), fine-tuned for 10 epochs with a fixed 60% *train*, 10% *val*, 30% *test* split. The Trie feature weights ($\lambda_F, \lambda_L, \lambda_R$) were set uniformly to 1/3. The test sets for the abrupt, incremental, and gradual drift scenarios followed the concept progressions shown in Fig. 3, and all experiments were executed under identical con-

figurations. Experiments ran on the Lonestar6 (LS6) system at TACC using a single NVIDIA A100 GPU (40GB), 64 CPU cores, and 64GB RAM.

6 Conclusion

This work introduced ***ODD*** (**Online Domain-Aware Decoding**), pioneering the *first inference-time, online domain-aware decoding framework* to mitigate concept drift without external retrieval or additional model training. *ODD* is defined by a *single-pass decoding architecture* powered by an *Adaptive Fusion Mechanism*. This mechanism dynamically balances LLM fluency with trie constraints by applying a runtime reward–penalty bias based on *disagreement* and *continuity* signals, ensuring structural correctness and real-time adaptation with near-zero latency overhead. The framework’s efficiency relies on its *lightweight prefix-trie* architecture. This trie stores tokenized placeholders, enabling fast $\mathcal{O}(L)$ updates, efficient $\mathcal{O}(L^2)$ retrieval, compact memory scaling, and near-zero latency via linear-time lookups during decoding. Empirically, using a unified *Online Domain Shift (ODS)* benchmark covering abrupt, incremental, and gradual drift, *ODD* demonstrated superior robustness across all scenarios. It outperformed baseline decoding methods on all NLG metrics, with an average absolute gain of **0.065** in ROUGE-L and a **13.6%** relative gain in Cosine Similarity, underscoring its ability to adapt reliably to dynamic linguistic environments.

References

1. Anderson, P., Fernando, B., Johnson, M., Gould, S.: Guided open vocabulary image captioning with constrained beam search. In: Proc. EMNLP ’17. pp. 936–945 (2017)
2. Anonymous: Odd online domain-aware llm decoding for continual domain evolution. <https://github.com/anonymous273800/ODD> (2025), GitHub repository
3. Bitext: Bitext telco llm chatbot training dataset (2023), available on Hugging Face: [bitext/Bitext-telco-llm-chatbot-training-dataset](https://huggingface.co/datasets/bitext/Bitext-telco-llm-chatbot-training-dataset)
4. Borgeaud, S.e.a.: Improving language models by retrieving from trillions of tokens. In: ICML ’22. pp. 2206–2240 (2022)
5. Brown, T., Mann, B., Ryder, N., Subbiah, M., Kaplan, J., et al.: Language models are few-shot learners. Adv. Neural Inf. Process. Syst. **33** (2020)
6. Chowdhery, A., Narang, S., Devlin, J., Bosma, M., et al.: Palm: Scaling language modeling with pathways. J. Mach. Learn. Res. **24**(240) (2023)
7. Dathathri, S., Madotto, A., Lan, J., et al.: Plug and play language models: A simple approach to controlled text generation. In: Proc. ICLR (2020)
8. De Lange, M., Aljundi, R., Masana, M., et al.: A continual learning survey: Defying forgetting in classification tasks. IEEE Trans. Pattern Anal. Mach. Intell. (2021)
9. Gama, J., Žliobaité, I., Bifet, A., Pechenizkiy, M., Bouchachia, A.: A survey on concept drift adaptation. ACM Comput. Surv. **46**(4) (2014)
10. Hu, E.J., Shen, Y., Wallis, P., Allen-Zhu, Z., Li, Y., Wang, S., Wang, L., Chen, W.: Lora: Low-rank adaptation of large language models. In: Proc. ICLR (2022)
11. Ji, Z., Lee, N., Frieske, R., Yu, T., et al.: Survey of hallucination in natural language generation. ACM Comput. Surv. **55**(12) (2023)
12. Khandelwal, U., Levy, O., Jurafsky, D., Zettlemoyer, L., Lewis, M.: Generalization through memorization: Nearest neighbor language models. In: Proc. ICLR (2020)

13. Krause, B., Gotmare, A., McCann, B., et al.: Gedi: Generative discriminator guided sequence generation. In: Findings EMNLP '21. pp. 4929–4952 (2021)
14. Lester, B., Al-Rfou, R., Constant, N.: The power of scale for parameter-efficient prompt tuning. In: Proc. EMNLP '21. pp. 3045–3059 (2021)
15. Lewis, P., Perez, E., Piktus, A., Petroni, F., et al.: Retrieval-augmented generation for knowledge-intensive nlp tasks. *Adv. Neural Inf. Process. Syst.* **33** (2020)
16. L'Hostis, G., Grangier, D., Auli, M.: Vocabulary selection strategies for neural machine translation. arXiv:1610.00072 (2016)
17. Li, X.L., Liang, P.: Prefix-tuning: Optimizing continuous prompts for generation. In: Proc. ACL-IJCNLP '21. pp. 4582–4597 (2021)
18. Lin, C.Y.: Rouge: A package for automatic evaluation of summaries. In: Text Summarization Branches Out. pp. 74–81 (2004)
19. Liu, A.e.a.: Dexperts: Decoding-time controlled text generation with experts and anti-experts. In: ACL-IJCNLP '21 (2021)
20. Liu, R., Zheng, G., Gupta, S., Gaonkar, R., Gao, C., Vosoughi, S., Shokouhi, M., Awadallah, A.H.: Knowledge infused decoding. In: Proc. ICLR (2023)
21. Maynez, J., Narayan, S., Bohnet, B., McDonald, R.: On faithfulness and factuality in abstractive summarization. In: Proc. ACL '20. pp. 1906–1919 (2020)
22. Meng, K., Bau, D., Andonian, A., Belinkov, Y.: Locating and editing factual associations in GPT. *Adv. Neural Inf. Process. Syst.* **35**, 17359–17372 (2022)
23. Meng, K., Sharma, A.S., Andonian, A.J., Belinkov, Y., Bau, D.: Mass-editing memory in a transformer. In: Proc. ICLR (2023)
24. Ouyang, L., Wu, J., Jiang, X., Almeida, D., et al.: Training language models to follow instructions with human feedback. *Adv. Neural Inf. Process. Syst.* **35** (2022)
25. Papineni, K., Roukos, S., Ward, T., Zhu, W.J.: Bleu: A method for automatic evaluation of machine translation. In: Proc. ACL '02. pp. 311–318 (2002)
26. Popović, M.: chrf: Character n-gram f-score for automatic MT evaluation. In: Proc. WMT '15. pp. 392–395 (2015)
27. Rajpurkar, P., Zhang, J., Lopyrev, K., Liang, P.: Squad: 100,000+ questions for machine comprehension of text. In: Proc. EMNLP '16. pp. 2383–2392 (2016)
28. Reimers, N., Gurevych, I.: Sentence-BERT: Sentence embeddings using siamese BERT-networks. In: Proc. EMNLP-IJCNLP '19. pp. 3982–3992 (2019)
29. Schick, T., Udupa, S., Schütze, H.: Self-diagnosis and self-debiasing: A proposal for reducing corpus-based bias in nlp. *TACL* **9**, 1408–1424 (2021)
30. Shi, H., Xu, Z., Wang, H., Qin, W., et al.: Continual learning of large language models: A comprehensive survey. *ACM Comput. Surv.* (2024)
31. Touvron, H., Lavril, T., Izacard, G., Martinet, X., et al.: Llama: Open and efficient foundation language models. arXiv:2302.13971 (2023)
32. Wu, Y., Wu, W., Yang, D., Xu, C., Li, Z.: Neural response generation with dynamic vocabularies. In: Proc. AAAI '18 (2018)
33. Yang, K., Klein, D.: Fudge: Controlled text generation with future discriminators. In: Proc. NAACL-HLT '21. pp. 3511–3535 (2021)
34. Yujian, L., Bo, L.: A normalized levenshtein distance metric. *IEEE Trans. Pattern Anal. Mach. Intell.* **29**(6), 1091–1095 (2007)
35. Zhang, T., Kishore, V., Wu, F., Weinberger, K.Q., Artzi, Y.: Bertscore: Evaluating text generation with bert. In: Proc. ICLR (2020)
36. Zhang, Y., Sun, S., Galley, M., et al.: Dialogpt: Large-scale generative pre-training for conversational response generation. In: ACL '20 System Demonstrations (2020)
37. Zhao, W.X., Zhou, K., Li, J., Tang, T., Wang, X., Hou, Y., Min, Y., Zhang, B., Zhang, J., Dong, Z., et al.: A survey of large language models. arXiv (2023)